

PH4103 Term Paper

Measurement of sub-milliohm resistance of a copper wire using an SR830 Lock-in Amplifier

Debayan Sarkar

22MS002

Diptanuj Sarkar

22MS038

Sabarno Saha

22MS037

Supervisor: Prof. Kamaraju Natarajan
Prof. Sourin Das

Date: 27 November 2025

Abstract

In this experiment, we make use of a lock-in amplifier to measure sub-milliohm resistance of a copper wire. To do this, we set up a two-probe measurement configuration where we pass a small AC current through the copper wire and measure the resulting voltage drop across it using the lock-in amplifier. We also characterize flicker noise ($1/f$ noise) observed in resistors and compare it with theoretical estimates. We also detail the basic working principle of a lock-in amplifier in this report.

Contents

1. The Lock-In Amplifier	3
1.1. Introduction	3
1.2. Working Principle	3
1.3. Core Blocks and Specifications of the SR830	5
1.3.1. Input and Reference Signals	5
1.3.2. Digital Low Pass Filters	5
1.3.3. Synchronous Filters	5
1.3.4. Dynamic Reserve	5
2. Flicker Noise	6
2.1. $\frac{1}{f^\alpha}$ noise from the superposition of relaxation processes	7
2.2. Can the fluctuations be infinitely large?	8
3. Sub-Milliohn Resistance Measurement	8
3.1. Procedure	8
3.2. Circuit Diagram	9
3.3. Parameters	9
3.4. Analysis	10
3.5. Resistance	11
3.6. Errors	11
3.7. Observations	13
3.8. Sources of Error	16

3.9. Conclusion	16
3.10. 1/f noise analysis	16
3.11. Working Principle	16
3.12. Parameters	17
3.13. Data analysis	18
3.14. Observations	19
References	20

1. The Lock-In Amplifier

1.1. Introduction

A lock-in amplifier is a type of amplifier that can extract a signal from an extremely noisy input. Generally, the signal we are trying to extract has a known carrier signal, i.e. a known frequency. The signal to noise ratio upto which we can reliably detect the target signal depends on the dynamic reserve of the instrument. For our experiments, we used Stanford Research Systems' Model SR830 DSP Lock-In Amplifier. As a DSP (Digital Signal Processor) lock-in amplifier, the SR830 performs most of it's core functions digitally, leading to a better performance than it's analog competitors. In the following section, we describe the workings of this amplifier in greater detail.

1.2. Working Principle

The core function that the lock-in amplifier performs, is *Phase Sensitive Detection*. Let's say the input signal we provide is $V_i(t) = V_0 \sin(\omega_i t + \varphi_i)$. The lock-in multiplies this signal with another reference signal, often provided by an internal oscillator. Let's say the reference sinusoidal signal is given by $V_r(t) = V_1 \sin(\omega_r t + \varphi_r)$. Note that both ω_r and φ_r of this internal oscillator are tunable parameters. After multiplying these two signals, we get

$$\begin{aligned} V_{\text{psd}}(t) &= V_i(t)V_r(t) \\ &= V_0V_1 \sin(\omega_i t + \varphi_i) \sin(\omega_r t + \varphi_r) \\ &= \frac{1}{2}V_0V_1 [\cos[(\omega_i - \omega_r)t + (\varphi_i - \varphi_r)] - \cos[(\omega_i + \omega_r)t + (\varphi_i + \varphi_r)]] \end{aligned} \quad (1.1)$$

As we can see, we end up with two different sinusoidal components. If $\omega_i = \omega_r$, then we end up with an oscillating AC signal at frequency $2\omega_r$ and a DC offset signal. If we now send this signal through a low pass filter (or equivalently take a time average of the signal), we will end up with just the DC signal, which from our calculations turns out to be,

$$V_{\text{lpf}} = \frac{1}{2}V_0V_1 \cos(\Delta\varphi) \quad (1.2)$$

Where $\Delta\varphi = \varphi_i - \varphi_r$, can be adjusted to 0 by setting $\varphi_r = \varphi_i$. The output of the low pass filter can then be scaled down by $\frac{1}{2}V_r$, and we finally end up with the output voltage of $V_{\text{out}} = V_0$. Note that it's not necessary that the input signal is a pure sinusoid. Infact, most of the times it will not be one.

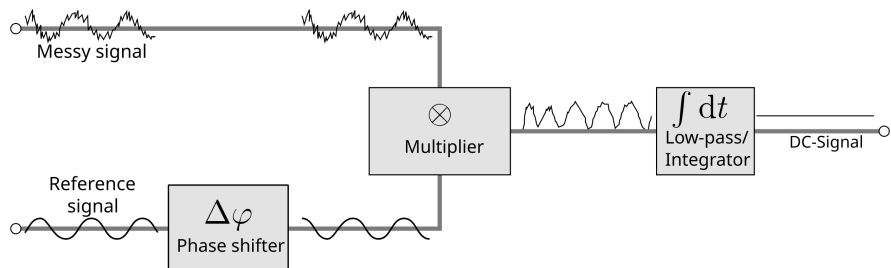


Figure 1: Schematic diagram of a Phase Sensitive Detector (Credits: Zelbear on Wikipedia)

We can use the lock-in amplifier to extract all the fourier components of the target signal at the reference frequency. To do this, the lock-in performs the calculation we just described, twice in the two quadratures by using a 90° phase shifted copy of the reference signal. It's better explained by this schematic diagram shown below.

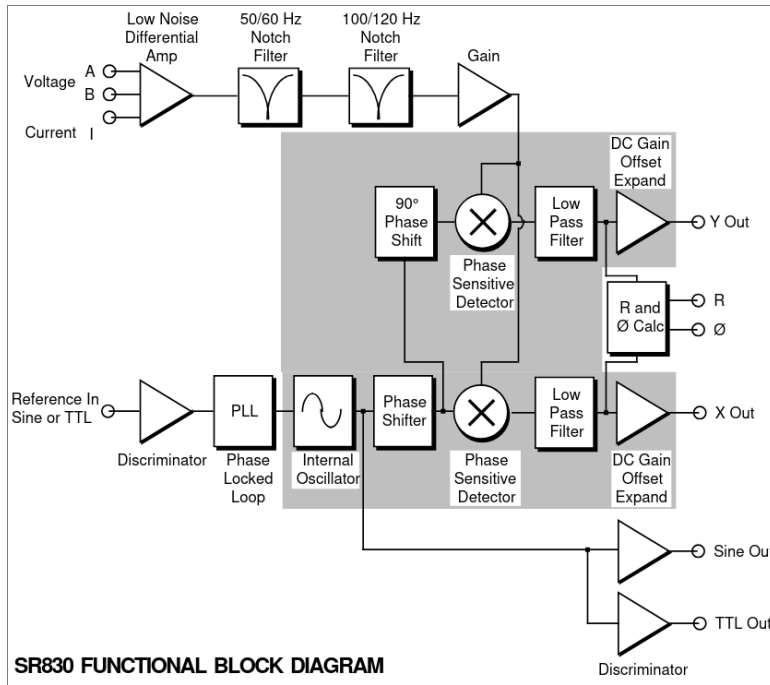


Figure 2: Schematic Diagram for the SR830 Lock-In Amplifier (Credits: Stanford Research Systems)

And the end of this process, we end up with two signals, X and Y , which correspond to the sin and cos quadratures of the signal respectively. The lock-in also calculates two other variables R and θ as

$$R = \sqrt{X^2 + Y^2} \quad (1.3)$$

$$\theta = \arctan\left(\frac{Y}{X}\right) \quad (1.4)$$

1.3. Core Blocks and Specifications of the SR830

In this section we describe the core blocks of the SR830 lock-in amplifier, along with the various specifications and available values for the adjustable parameters in those blocks. Below is an image of the front-panel of the SR830.



Figure 3: Front Panel of the SR830 (Credits: Stanford Research Systems)

As mentioned before, all the core functionalities in an SR830 are done using a DSP (Digital Signal Processor).

1.3.1. Input and Reference Signals

The analog input signal is digitised, into a 20 bits, 256 kHz sample-rate digital signal. After this, all the computation for phase sensitive detection that we discussed before, is done digitally using the DSP. Even the reference signal is digitally synthesized. The SINE OUT signal is just that digitally synthesized signal, passed through a Digital to Analog Converter. For the reference signal, we can adjust the Phase, Frequency and Amplitude.

1.3.2. Digital Low Pass Filters

The SR830 uses digital filters, which again are implemented using the DSP. Since the filters are digital, we are not limited to just two stages of filtering. Instead, each PSD can be followed by upto 4 filters, giving us roll-offs ranging from 6dB/Octave to 24dB/Octave. The filter has a adjustable roll-off, and an adjustable time constant. The time constant of the filter is just $\frac{1}{2\pi f}$ where f is the -3dB frequency. The time constants range from $1\mu\text{s}$ to 300s .

1.3.3. Synchronous Filters

Recall that the output of our PSD originally gave us a DC signal, and a signal at twice the detection frequency. If our detection frequency (say f) is too small, then the $2f$ frequency might be harder to filter out. The lower $2f$ gets, the higher we must set the time constant and roll-off of our low pass filter. However, SR830 has synchronous filtering. The synchronous filter averages the PSD output over a period of the reference signal. Which means, all the harmonics of the detection frequency f are notched out. If our signal was perfectly clean, even the need for the Low Pass Filtering stage is removed. We only use the synchronous filter for detection frequencies under 200 Hz. Above that, removing the $2f$ frequency using normal filter stages is feasible.

1.3.4. Dynamic Reserve

TODO

2. Flicker Noise

After the invention of the “thermionic tube” amplifiers in 1921, C.A. Hartmann attempted an experiment to verify Schottky’s formula for the shot noise spectral density [1]; Hartmann failed, and it was J. B. Johnson (of Johnson-Nyquist fame) who measured the white noise spectrum. However, Johnson also measured an unexpected “flicker noise” at low frequencies. This is shown in the following diagram:

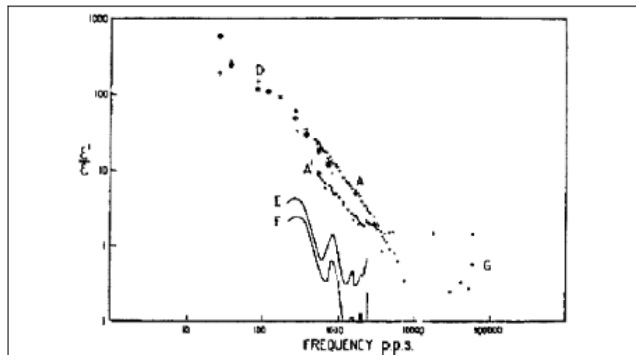


Fig. 6. Frequency variation for tube No. 2, coated filament; same data as in Fig. 4 plotted to a frequency scale; curves E and F give Hartmann's results for 2 m-a. and 20 m-a.; points G were obtained with less steady measuring circuit.

Figure 1: the spectral density observed by J. B. Johnson, as shown in his original paper [3]. The vertical scale represents the observed noise power density divided by the theoretical shot noise power density; the horizontal scale is the frequency in Hz.

Figure 4: (Source: [2])

It was soon found that such “flicker noise” is found in many systems. The observed spectral density of flicker noise is quite variable, as it behaves like $\frac{1}{f^\alpha}$, where $\alpha \in [0.5, 1.5]$, and this behaviour extends over several frequency decades.

The appearance of power laws in the theory of critical phenomena, and the work of B. Mandelbrot on fractals [3]; seemed to indicate something universal with noise of this spectral signature.

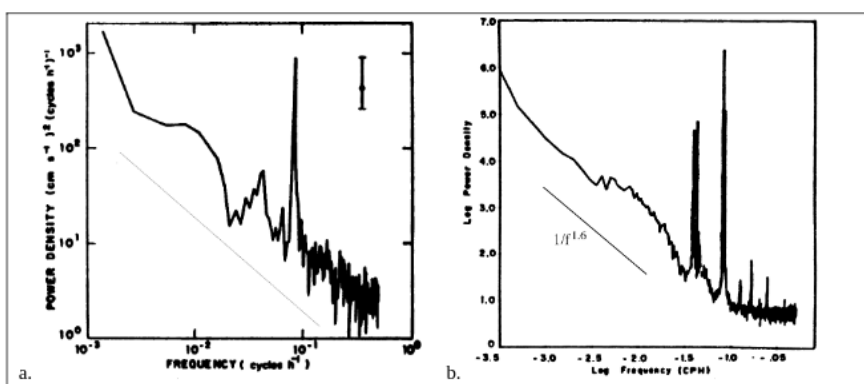


Figure 2: a. power spectrum of the east-west component of ocean current velocity [7]; the straight line shows the slope of a $1/f$ spectrum. b. sea level at Bermuda: this is $1/f^\alpha$ spectrum with $\alpha \approx 1.6$ [8].

Figure 5: (Source: [2]; Some examples of $1/f$ noise)

2.1. $\frac{1}{f^\alpha}$ noise from the superposition of relaxation processes

Some of the early explanations of the appearance of $\frac{1}{f^\alpha}$ noise in vacuum tubes due to Johnson [4]; and Schottky [5]; aligned along these lines: There is a contribution to the vacuum tube current from the cathode surface trapping sites, which release electrons according to a simple exponential relaxation law:

$$N(t) = N_0 e^{-\lambda t}, t \geq 0 \quad (2.1)$$

The Fourier transform of a single exponential relaxation process is given by:

$$F(\omega) = \int_{-\infty}^{\infty} N(t) e^{-i\omega t} dt = N_0 \int_0^{\infty} e^{-(\lambda+i\omega)t} dt = \frac{N_0}{\lambda + i\omega} \quad (2.2)$$

If we image a sequence of such pulses, given by:

$$N(t, t_k) = N_0 e^{-\lambda(t-t_k)}, t \geq t_k \quad (2.3)$$

where $N(t, t_k) = 0$ for $t < t_k$. Taking the Fourier transform of this,

$$F(\omega) = \int_{-\infty}^{\infty} \sum_k N(t, t_k) e^{-i\omega t} dt = \frac{N_0}{\lambda + i\omega} \sum_k e^{i\omega t_k} \quad (2.4)$$

Which represents a spectrum given by:

$$S(\omega) = \lim_{T \rightarrow \infty} \frac{1}{T} \langle |F(\omega)|^2 \rangle = \frac{N_0^2}{\lambda^2 + \omega^2} \lim_{T \rightarrow \infty} \frac{1}{T} \langle \left| \sum_k e^{i\omega t_k} \right|^2 \rangle = \frac{N_0^2 n}{\lambda^2 + \omega^2} \quad (2.5)$$

Where n is the average pulse rate, and the average indicated is the ensemble average. This spectrum is nearly flat at small frequencies, and after a transition region it becomes proportional to $\frac{1}{\omega^2}$ at high frequencies. This does happen at high frequencies, and is often called “red noise”. But it does not explain the data collected by Johnson, i.e. the $1/f$ noise.

As a next step, we can consider a superposition of such relaxation processes with a distribution of relaxation rates [6] λ . Let us assume that this distribution is uniform in the range $\lambda \in [\lambda_1, \lambda_2]$, and that the amplitude of each pulse remains the same. With this, we can derive a spectrum:

$$S(\omega) = \frac{1}{\lambda_1 - \lambda_2} \int_{\lambda_1}^{\lambda_2} \frac{N_0^2 n}{\lambda^2 + \omega^2} d\lambda = \frac{N_0^2 n}{\omega(\lambda_2 - \lambda_1)} \left[\arctan\left(\frac{\lambda_2}{\omega}\right) - \arctan\left(\frac{\lambda_1}{\omega}\right) \right] \quad (2.6)$$

So, in different regimes, we have:

$$1. \quad S(\omega) = N_0^2 n, 0 < \omega \ll \lambda_1 \ll \lambda_2 \quad (2.7)$$

$$2. \quad S(\omega) = \frac{N_0^2 n \pi}{2\omega(\lambda_2 - \lambda_1)}, \lambda_1 \ll \omega \ll \lambda_2 \quad (2.8)$$

$$3. \quad S(\omega) = \frac{N_0^2 n}{\omega^2}, \lambda_1 \ll \lambda_2 \ll \omega \quad (2.9)$$

![[Pasted image 20251127004742.png]] (Source: [2];)

Numerical studies have shown that this spectrum is relatively insensitive to small deviations from a perfectly uniform distribution of relaxation rates λ [2].

Now, if we distribute the relaxation rates according to a distribution given by:

$$dP(\lambda) = \frac{A}{\lambda^\beta} d\lambda, \lambda \in (\lambda_1, \lambda_2) \quad (2.10)$$

we can still calculate the spectrum integral exactly, as summarised by van der Ziel [7];. The results are:

$$S(\omega) \propto \int_{\lambda_1}^{\lambda_2} \frac{1}{\lambda^2 + \omega^2} \frac{d\lambda}{\lambda^\beta} \quad (2.11)$$

Where we get:

$$1. \quad \beta = 1 \implies S(\omega) = \frac{1}{\omega^2} \left[\ln\left(\frac{\lambda}{\sqrt{\lambda^2 + \omega^2}}\right) \right]_{\lambda_1}^{\lambda_2} \quad (2.12)$$

2.

$$\beta \neq 1 \implies S(\omega) = \frac{\lambda^{1-\beta}}{(1-\beta)\omega^2} F\left[\left(\frac{1-\beta}{2}, 1, \frac{1-\beta}{2}, -\frac{\lambda^2}{\omega^2}\right)\right]_{\lambda_1}^{\lambda_2} \quad (2.13)$$

Here,

$$F(a, b, c, d) = \frac{\Gamma(c)}{\Gamma(b)\Gamma(c-b)} \int_0^1 t^{b-1} (1-t)^{c-b-1} (1-td)^{-a} dt \quad (2.14)$$

Which is a hypergeometric function. We do not have to use the exact expression for the spectrum, as it is possible to approximate in the region $\lambda \in (\lambda_1, \lambda_2)$ as:

$$S(\omega) \propto \int_{\lambda_1}^{\lambda_2} \frac{1}{\lambda^2 + \omega^2} \frac{d\lambda}{\lambda^\beta} = \frac{1}{\omega^{1+\beta}} \int_{\lambda_1}^{\lambda_2} \frac{1}{1 + \frac{\lambda^2}{\omega^2}} \frac{d\frac{\lambda}{\omega}}{(\frac{\lambda}{\omega})^\beta} = \frac{1}{\omega^{1+\beta}} \int_{\lambda_1/\omega}^{\lambda_2/\omega} \frac{1}{1+x^2} \frac{dx}{x^\beta} \quad (2.15)$$

Which may be simplified to:

$$S(\omega) \propto \frac{1}{\omega^{1+\beta}} \int_0^\infty \frac{1}{1+x^2} \frac{dx}{x^\beta} \propto \frac{1}{\omega^{1+\beta}} \quad (2.16)$$

Which is the $\frac{1}{f^\alpha}$ spectra that we expected.

2.2. Can the fluctuations be infinitely large?

In most systems, it is seen that the $1/f$ behaviour continues for many decades in frequency - making it impossible to determine λ_1 and λ_2 . Data from Pellegrini et. al shows this for voltage fluctuations in thin film resistors, where the behaviour is observed over 6 frequency decades. [8]; But this is a problem, as if this behaviour continues down to zero frequency we would have infinite integrated fluctuation as shown by:

$$\int_0^\infty S(f) df \propto \lim_{f_1 \rightarrow 0, f_2 \rightarrow \infty} \int_{f_1}^{f_2} \frac{1}{f} df = \lim_{f_1 \rightarrow 0, f_2 \rightarrow \infty} \ln \frac{f_2}{f_1} \quad (2.17)$$

Which obviously diverges. This is also true for any $\frac{1}{f^\alpha}$ spectra. Flinn [9]; produced a simple argument that shows that such a blow-up is not physical and there is no need to worry about it. Note that the integrated fluctuation for $1/f$ noise is always the same for every frequency decade. Now, the lowest observable frequency in the universe is the inverse of the lifetime of the Universe, which is approximately $10^{-17} Hz$. On the other hand, if we take the Planck time as the smallest observable time, we get a frequency of approximately $10^{43} Hz$. So, there are a total of 59 frequency decades that are observable, which means that the highest total possible fluctuation can only be 59 times the total fluctuation between $1 Hz$ and $10 Hz$.

3. Sub-Milliohn Resistance Measurement

In this experiment, we aim to measure the sub-milliohm resistance of a copper wire using an SR830 Lock-in Amplifier, using the four-probe method to minimize contact resistance effects. This experiment was proposed in its two probe configuration in [10]. We extend this to a four-probe configuration for better accuracy.

3.1. Procedure

1. Connect the copper wire sample in a four-probe configuration to the SR830 Lock-in Amplifier.
2. Our lock-in amplifier's was inconsistent in using an external current source using **REF IN**. It failed to use the external trigger of the signal generator. So we shall, instead use the signal generated by the **SINE OUT** of the lock-in amplifier itself to drive current through the sample.
3. The circuit used is given below in Figure 6, using voltage divider, we obtain the resistance of the wire R_w .
4. We set the amplitude of the lock-in amplifier to some reference value, say 2.5 V for our case.

5. We set the time constant of the lock-in amplifier and the sensitivity appropriately to get a stable reading.
6. We **AUTO PHASE** and **AUTO GAIN** the lock-in amplifier to optimize the phase and gain settings, such that the gain does
7. We record the measurements using a GPIB cable and python scripts using the **pyvisa** library.
8. We vary the frequency of the lock-in amplifier from 10 Hz to 100 kHz, and record the voltage across the inner probes.
9. For each frequency, after setting the frequency, we wait for several time constants and then record the voltage reading and the voltage fluctuations.
10. The Plots are then taken and analyzed.

3.2. Circuit Diagram

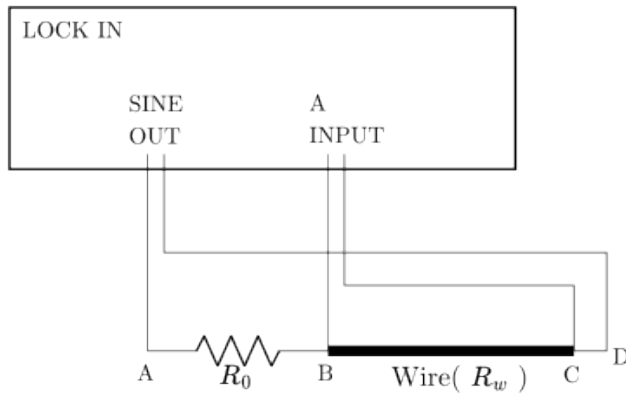


Figure 6: Circuit diagram for four-probe resistance measurement using SR830 Lock-in Amplifier.

The Four probe configuration uses the **SINE OUT** of the lock-in amplifier to drive current through the outer probes A and D. The voltage across the inner probes B and C is measured using the differential input of the lock-in amplifier. We now infer wire resistance R_w using the voltage divider formula. The current I through the wire is given by:

$$I = \frac{V_A - V_C}{R_0 + R_w} = \frac{V_B - V_C}{R_w} \quad (3.1)$$

Also note that $V_C = 0$, since it is the ground reference for the lock-in amplifier. Using this, we can derive the expression for R_w as:

$$\begin{aligned} \frac{V_A - V_C}{R_0 + R_w} &= \frac{V_B - V_C}{R_w} \\ \Rightarrow R_w &= \frac{V_B}{V_A} \frac{R_0}{1 + \frac{R_w}{R_0}} \\ \Rightarrow R_w &\approx \frac{V_B}{V_A} R_0 \text{ (since } R_w \ll R_0) \end{aligned} \quad (3.2)$$

For our experiment, we choose $R_0 = 1\text{kHz}$, which is much larger than the expected resistance of the copper wire, which is in the sub-milliohm range. This approximation is correct upto and order of $10^{-6}\Omega$.

3.3. Parameters

The parameters used in the experiment are tabulated below:

1. Reference Voltage Amplitude: 2.5 V
2. Reference Frequency: 10 Hz to 100 kHz (varied)
3. Series Resistor R_0 : 1 k Ω
4. Time Constant: 1 s
5. Sensitivity: 24 dB/oct

3.4. Analysis

The recorded voltage across the inner probes is used to calculate the resistance of the copper wire using the derived formula. The resistance values are plotted against the frequency to observe any frequency dependence. We collected 4 datasets. Note that we have plotted the voltages of R, X, Y from with the frequency in the log scale.

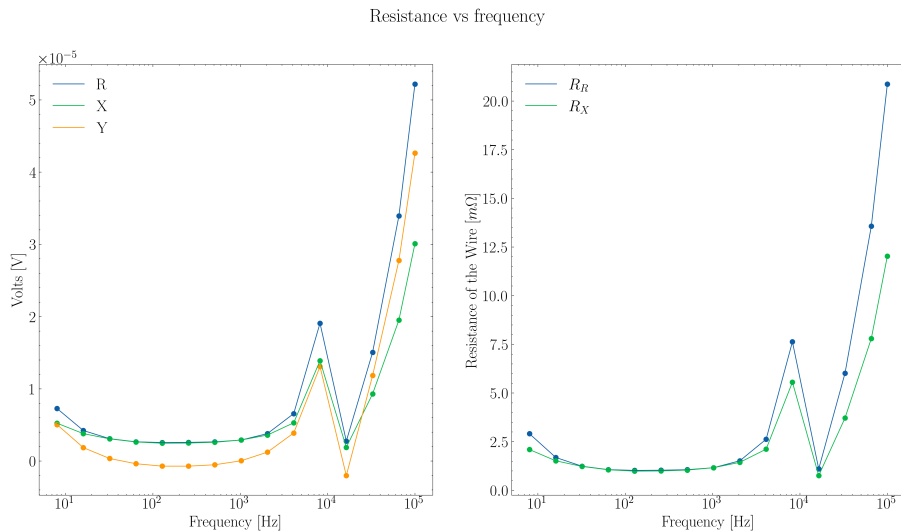


Figure 7: Voltage vs Frequency plot.

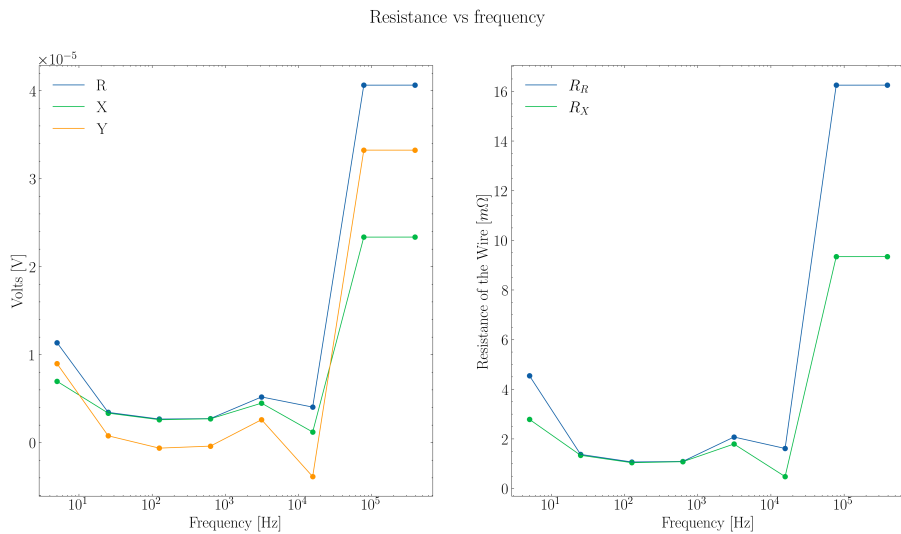
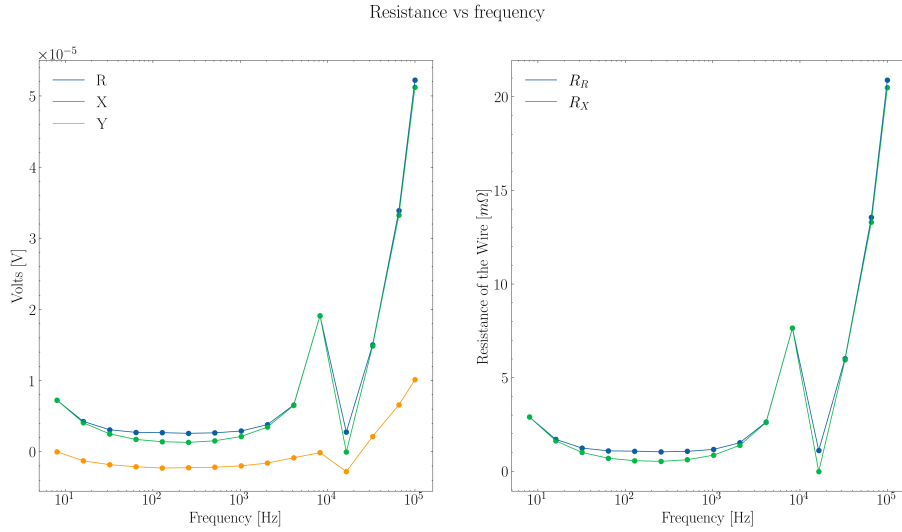
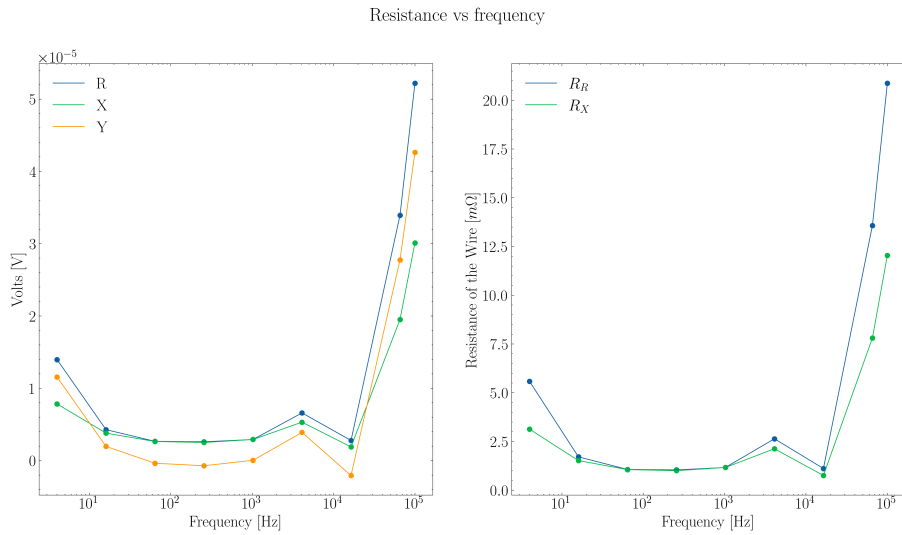


Figure 8: Voltage vs Frequency plot.

**Figure 9:** Voltage vs Frequency plot.**Figure 10:** Voltage vs Frequency plot.

3.5. Resistance

3.6. Errors

The voltage plots have been calculated with error bars, which are derived from the voltage fluctuations recorded during the experiment. The error bars have been scaled by a factor of 100 for better visibility in the plots.

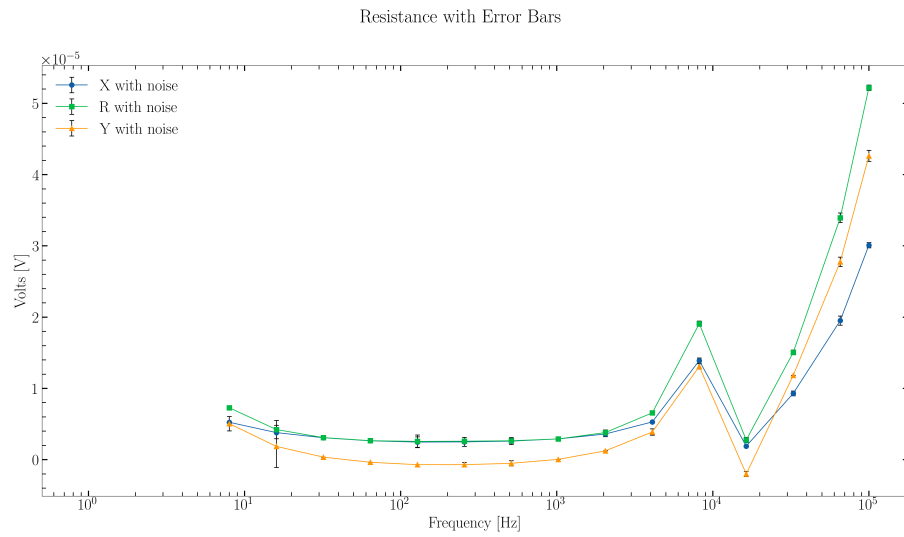


Figure 11: Voltage vs Frequency plot with errorbars.

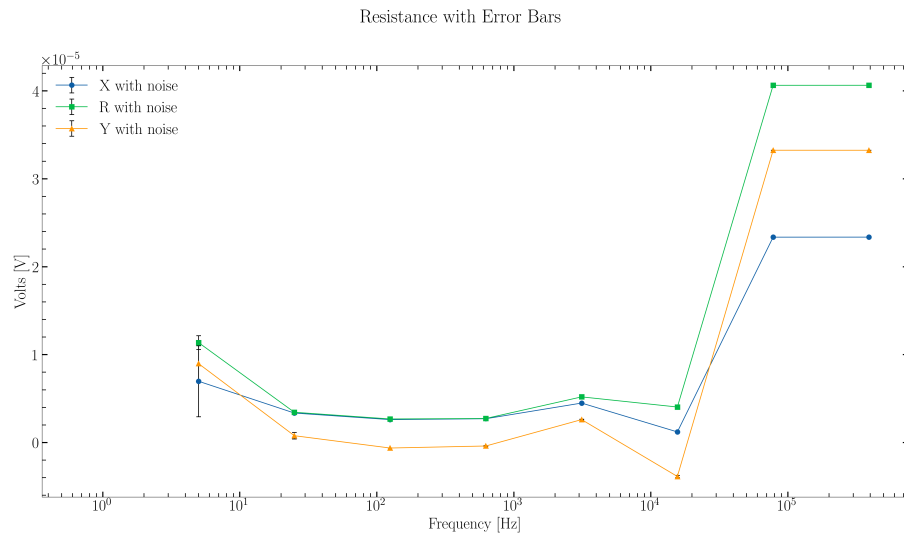


Figure 12: Voltage vs Frequency plot with errorbars.

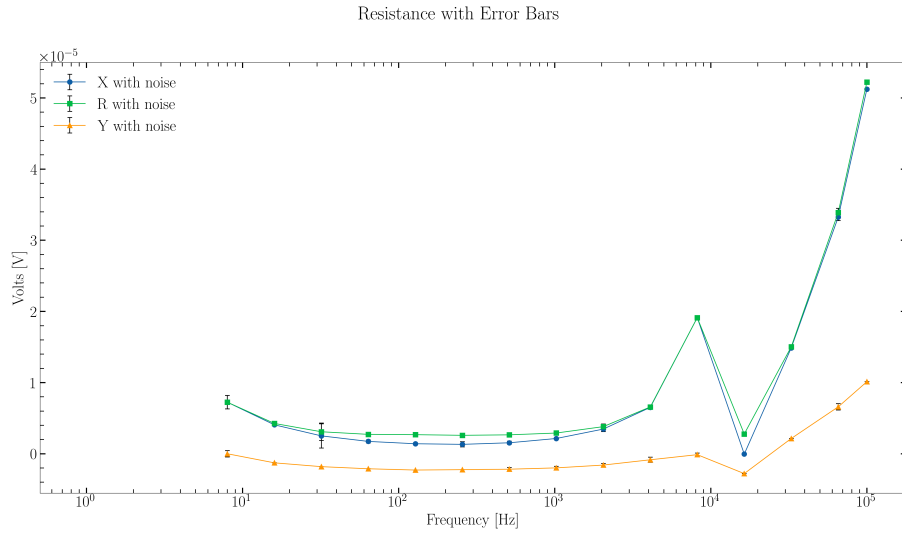


Figure 13: Voltage vs Frequency plot with errorbars.

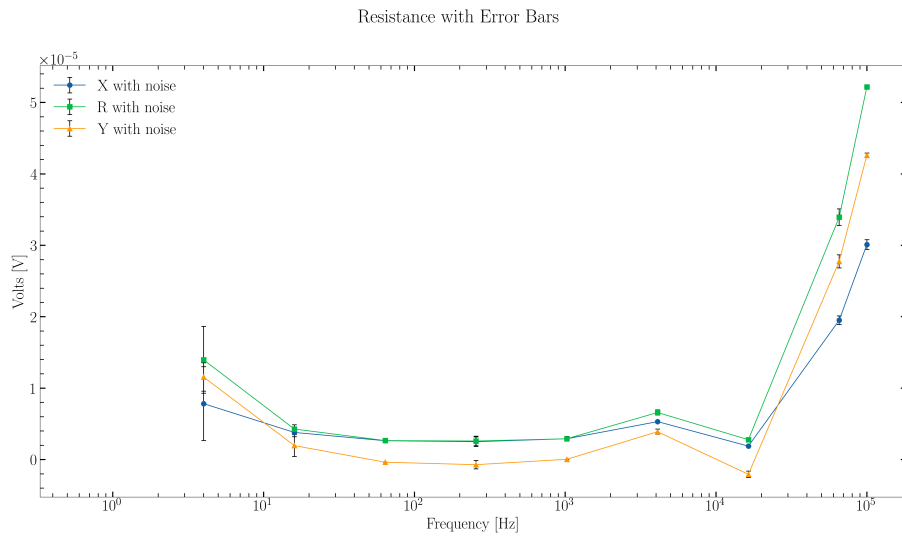


Figure 14: Voltage vs Frequency plot with errorbars.

3.7. Observations

The resistance values calculated from the voltage measurements are in the sub-milliohm range, as expected for a copper wire. Nevertheless there are some features of the graphs that are interesting.

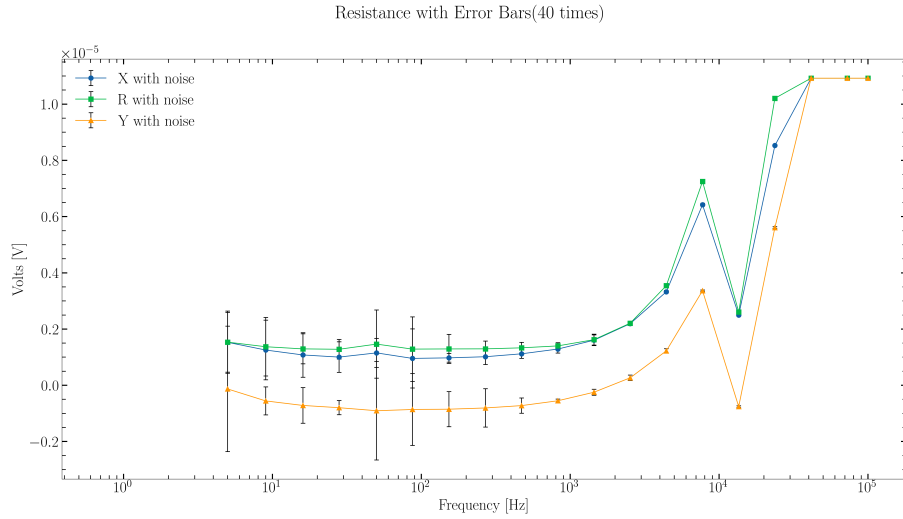


Figure 15: Voltage vs Frequency plot with errorbars.

Consider the graph above. At the 50 Hz frequency, we see a spike in voltage, along with a spike in voltage fluctuations. This is likely due to the power line interference at 50 Hz, since AC power lines operate at this frequency. The interference can introduce noise into the measurements, leading to increased voltage readings and fluctuations.

A much more interesting feature is the dip in voltage at around 10 kHz. This feature is present in all the datasets, albeit at slightly different frequencies. We name this unexpected effect “The Bermuda Bandwidth”. This effect is unexpected, and we do not have a clear explanation for it. The dips can be observed in all voltage components R, X, Y, θ .

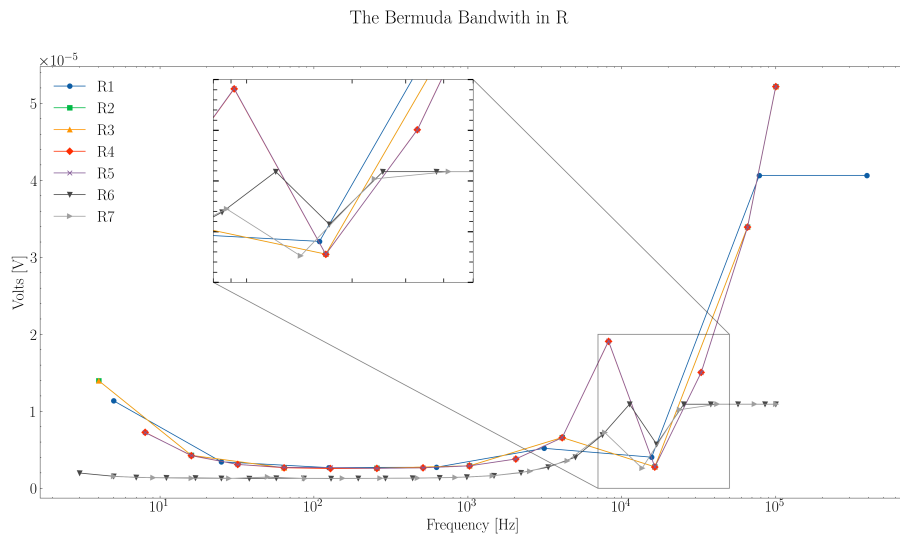


Figure 16: Voltage vs Frequency plot showing the dip.

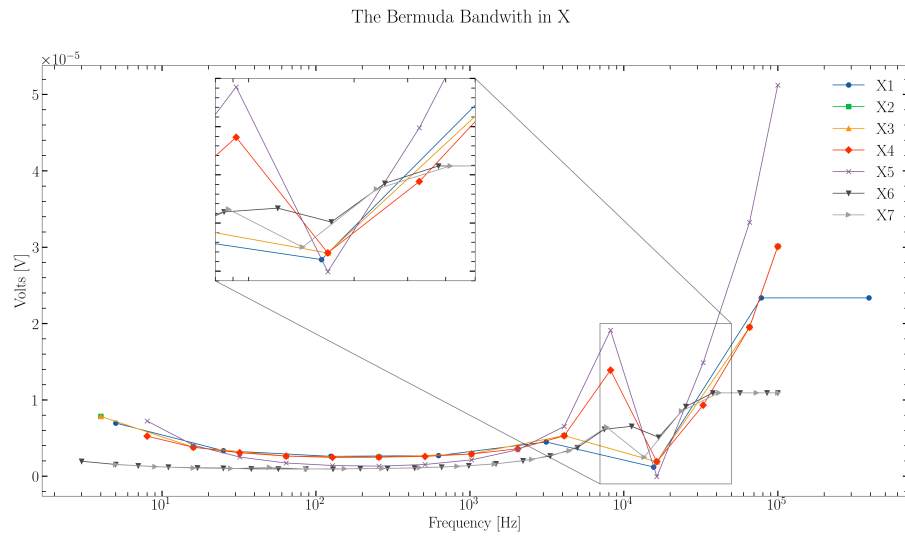


Figure 17: Voltage vs Frequency plot showing the dip.

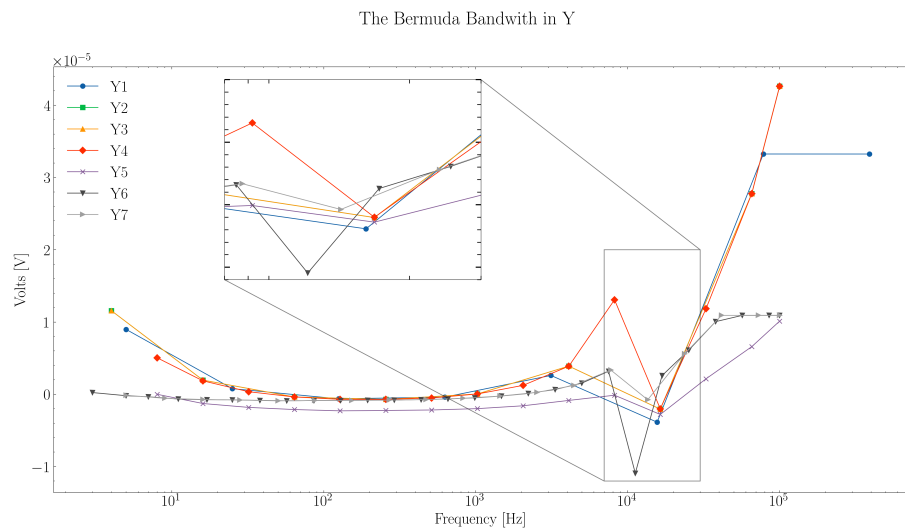


Figure 18: Voltage vs Frequency plot showing the dip.

The effect is however most pronounced in the phase angle theta plot.

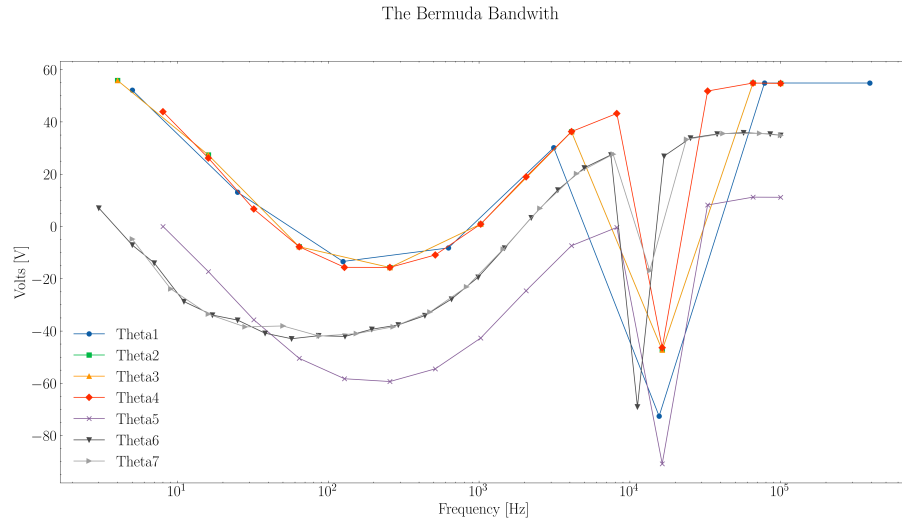


Figure 19: Voltage vs Frequency plot showing the dip.

3.8. Sources of Error

3.9. Conclusion

In this experiment, we successfully measured the sub-milliohm resistance of a copper wire using a four-probe configuration with an SR830 Lock-in Amplifier. The results indicate that the resistance values are in the expected range.

One hint about the next part of our report can be gleaned from the fact that the errorbars are larger in the lower frequency domain, which leads to our next section on $\frac{1}{f}$ noise analysis.

3.10. 1/f noise analysis

In this section, we analyze the voltage fluctuations recorded during the resistance measurements to investigate the presence of $\frac{1}{f}$ noise, also known as flicker noise. This type of noise is characterized by a power spectral density that is inversely proportional to the frequency, and it is commonly observed in electronic devices and materials.

In resistors, we model this noise using the relaxation model derived in the theory section. Resistors have defects that can trap and release charge carriers, leading to fluctuations in resistance and voltage, which cause the observed $\frac{1}{f}$ noise.

3.11. Working Principle

Generally, $\frac{1}{f}$ noise can be characterised by its power spectral density (PSD), which is obtained from the Fourier transform of the autocorrelation function of the voltage signal. However for a lockin amplifier, the voltage fluctuations die down rapidly due to the filtering with specifications mentioned in the manual. Therefore, we directly analyse the variance of the voltage signal as a function of frequency to identify the presence of $\frac{1}{f}$ noise. To do that, we must analyse why that works and how erroneous it is.

Let the noise be denoted by the variable $x(t)$. The power spectral density $S(f)$ is defined as:

$$S(f) = \lim_{T \rightarrow \infty} \frac{1}{T} |\hat{x}_T(f)|^2 \quad (3.3)$$

where $\hat{x}_T(f)$ is the Fourier transform of the signal $x(t)$ over a time interval T . The average power in a frequency band $[f_1, f_2]$ is then given by:

$$\langle P \rangle \propto \int_{f_1}^{f_2} S(f) df \quad (3.4)$$

We assume that the lock-in does not have an ideal rectangular filter, but rather a band-pass filter with a finite bandwidth Δf around the reference frequency f . Then we can relate the average voltage fluctuations in the bandwidth $[f, f + \Delta f]$ to the power spectral density. The average power in this band is:

$$\langle P \rangle_f \propto \int_f^{f+\Delta f} S(f) df \quad (3.5)$$

If we assume that the noise follows a $\frac{1}{f}$ dependence, i.e. $S(f) = \frac{A}{f}$, where A is a constant, Assuming that Δf is small compared to f , we can approximate the integral as:

$$\langle P \rangle_f \propto \frac{A}{f^2} \Delta f \quad (3.6)$$

Note that P here is the power of the noise signal. One assumption here is that the noise voltage also follows the same dependence, i.e. $V^2 \propto P$. Therefore, we can write:

$$\langle V_{\text{noise}}^2 \rangle_f \propto \frac{1}{f^2} \quad (3.7)$$

Note for our case, the signal is the average voltage $\langle V \rangle$, then the Noise voltage is given by $V_{\text{noise}} = V - \langle V \rangle$. We can thus see that,

$$\delta V_{\text{noise}} = \sqrt{\langle V_{\text{noise}}^2 \rangle} \propto \frac{1}{f} \quad (3.8)$$

The errors in this approximation arise as powers of $\frac{\Delta f}{f}$. So one way to mitigate the error due to approximation is to ignore lower values of f .

3.12. Parameters

The parameters used for the $\frac{1}{f}$ noise analysis are as follows:

1. Reference Voltage Amplitude: 10 mV
2. Reference Frequency: 10 Hz to 100 kHz (varied)
3. Series Resistor R_0 : 1 kΩ
4. Time Constant: 10 ms
5. Sensitivity: 6 dB/oct

The experimental procedure is the exact same as described in the previous section. Except here, we focus on recording the voltage fluctuations at each frequency setting of the lock-in amplifier.

3.13. Data analysis

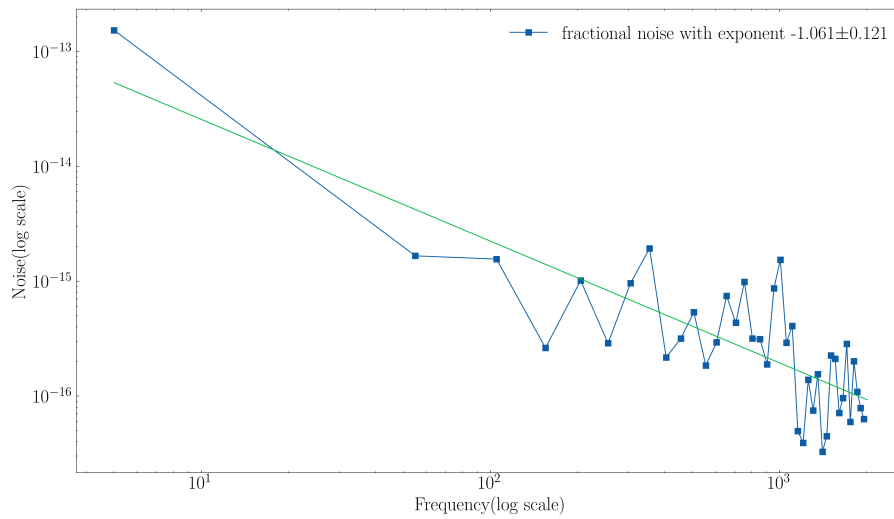


Figure 20: Noise Voltage vs Frequency plot with the sync filter turned on.

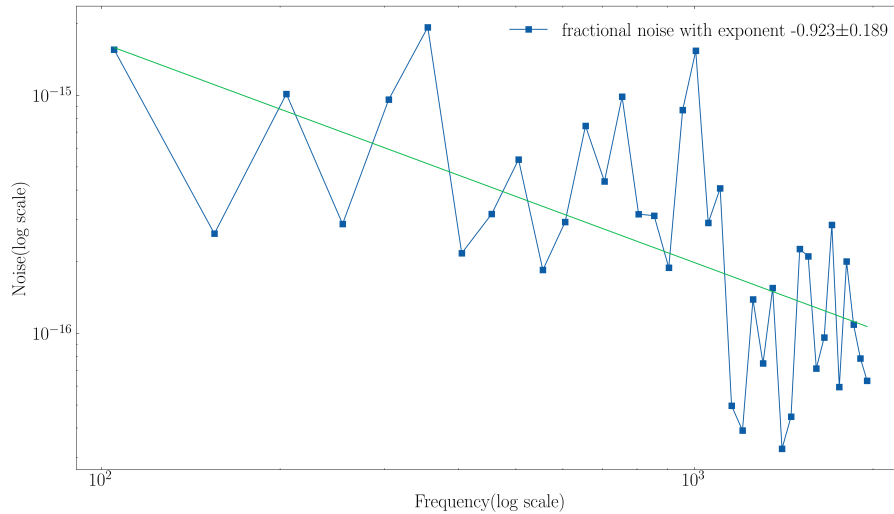


Figure 21: Noise Voltage vs Frequency plot with the sync filter turned on and initial datapoints removed.

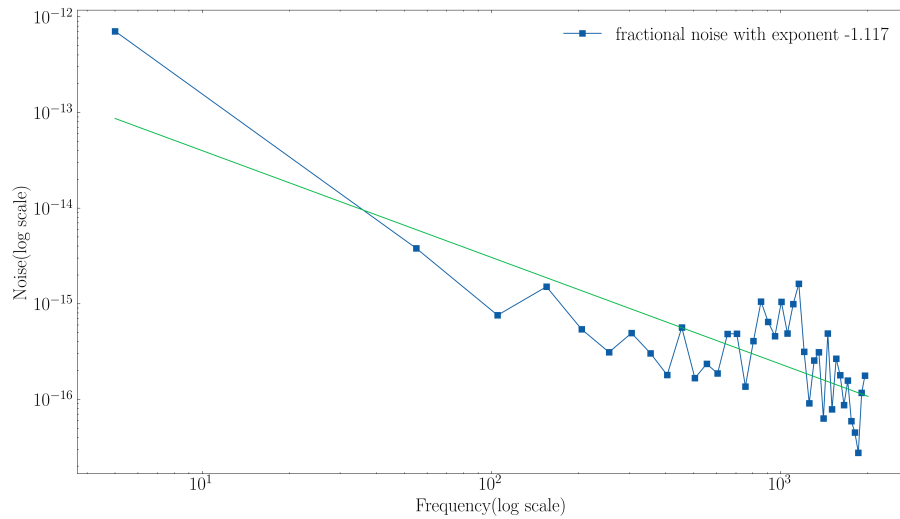


Figure 22: Noise Voltage vs Frequency plot with the sync filter turned off.

3.14. Observations

We observe $\frac{1}{f}$ noise in the data both in datasets with the sync filter turned on and the sync filter turned off. Th

References

- [1] C. A. Hartmann, “Über die Bestimmung des elektrischen Elementarquantums aus dem Schrotteffekt,” *Annalen der Physik*, vol. 65, p. 51–?, 1921.
- [2] E. Milotti, “1/f noise: a pedagogical review.” [Online]. Available: <https://arxiv.org/abs/physics/0204033>
- [3] B. B. Mandelbrot, *Fractals: Form, Chance and Dimension*. W. H. Freeman, Co., 1977.
- [4] J. B. Johnson, “The Schottky Effect in Low Frequency Circuits,” *Physical Review*, vol. 26, no. 1, pp. 71–85, Jul. 1925, doi: [10.1103/physrev.26.71](https://doi.org/10.1103/physrev.26.71).
- [5] W. Schottky, “Über spontane Stromschwankungen in verschiedenen Elektrizitätsleitern,” *Physical Review*, vol. 28, no. 1, pp. 74–100, Jul. 1926, doi: [10.1103/physrev.28.74](https://doi.org/10.1103/physrev.28.74).
- [6] J. Bernamont, “Fluctuations in the resistance of thin films,” *Proceedings of the Physical Society*, vol. 49, no. 4S, pp. 138–139, Aug. 1937, doi: [10.1088/0959-5309/49/4s/316](https://doi.org/10.1088/0959-5309/49/4s/316).
- [7] A. Van Der Ziel, “Flicker Noise in Electronic Devices,” in *Advances in Electronics and Electron Physics*, Elsevier, 1979, pp. 225–297. doi: [10.1016/s0065-2539\(08\)60768-4](https://doi.org/10.1016/s0065-2539(08)60768-4).
- [8] B. Pellegrini, R. Saletti, P. Terreni, and M. Prudenziati, “ $\frac{1}{f^\gamma}$ noise in thick-film resistors as an effect of tunnel and thermally activated emissions, from measures versus frequency and temperature”, *Physical Review B*, vol. 27, no. 2, pp. 1233–1243, Jan. 1983, doi: [10.1103/physrevb.27.1233](https://doi.org/10.1103/physrevb.27.1233).
- [9] I. FLINN, “Extent of the 1/f Noise Spectrum,” *Nature*, vol. 219, no. 5161, pp. 1356–1357, Sep. 1968, doi: [10.1038/2191356a0](https://doi.org/10.1038/2191356a0).
- [10] K. G. Libbrecht, E. D. Black, and C. M. Hirata, “A basic lock-in amplifier experiment for the undergraduate laboratory,” *American Journal of Physics*, vol. 71, no. 11, pp. 1208–1213, Oct. 2003, doi: [10.1119/1.1579497](https://doi.org/10.1119/1.1579497).